

Nonlinear vibration and of the Duffing oscillator to parametric excitation with time delay feedback

Y. A. Amer · A. T. EL-Sayed · A. A. Kotb

Received: 16 August 2014 / Accepted: 7 May 2016 / Published online: 23 May 2016
© Springer Science+Business Media Dordrecht 2016

Abstract The aim of this paper was to study the nonlinear vibrations of a parametric excited Duffing oscillator with time delay feedback. At some values of the time delay can be used to suppress the vibration of the nonlinear system. The method of multiple scales perturbation is applied to obtain the analytical solution of the system and the frequency response equation near sub-harmonic resonance case. The stability of the obtained nonlinear solution is studied and solved numerically. The effects of the different parameters of the system behavior are investigated. Analytical solution in this paper is in good agreement with the numerical simulation.

Keywords Duffing oscillator · Multiple scales perturbation · Sub-harmonic resonance · Time delay · Stability

1 Introduction

Vibration occurring in most dynamical system can be controlled to decrease the risk of disturbance, damage and destruction of this dynamical system. We control these risks by different method of vibration control as passive and active control or by using time delay. The nonlinear system with time delays has been an important topic of research over the last decade. El-Bassiouny and El-kholy [1] investigated the primary and sub-harmonic resonances of a nonlinear single-degree-of-freedom system under feedback control with a time delay. The analytical solution studied by using the averaging method and multiple scales method. They obtained that when the time delay is increased the response amplitude loses stability. El-Gohary and El-Ganaini [2,3] presented the vibration reduction of hinged–hinged beam under piezoelectric absorber using time delay. The system is studied when subjected to different types of excitation forces at simultaneous resonance condition, where the system damage is probable. They illustrated that the time delay absorber is more effective than ordinary absorber and the delay time is an important factor in selecting the absorber. Saeed et al. [4] illustrated the effects of the time delay saturation-based controller to suppress the vibrations of nonlinear beam. From the results obtained that at specific values of time delays the controller’s amplitude can be reduced for the excitation frequencies smaller than the main system’s natural frequency.

Y. A. Amer
Department of Mathematics, Faculty of Science, Zagazig University, Zagazig, Egypt

A. T. EL-Sayed
Department of Basic Sciences, Modern Academy for Engineering and Technology, Maadi, Egypt

A. A. Kotb (✉)
Department of Mathematics, Faculty of Science, Damietta University, Damietta, Egypt
e-mail: kotbmath2010@yahoo.com

El-Sayed and Bauomy [5] studied the effect of time delay absorber on the helicopter blade flapping system when subjected to multi-parametric excitation forces. The time delay absorber reduction the high amplitude of the nonlinear system using the averaging method when the optimum delay time ranges is $\tau \leq 0.004$. Nbandjo et al. [6] discussed the control of vibration, snap-through instability and horse-shoe chaos in a double-well Duffing oscillator subjected to an external excitation. The effects of the time delay between the motion of the oscillator and the action of the control are illustrated. Also, conclusion described that the best estimation of the optimal parameters for the efficiency of the control should not neglect the effects of time delay. Zhao and Xu [7] considered the delayed feedback control in a two-degree-of-freedom nonlinear system with external excitation. At some values of the delay the dynamical behaviors became complex when the gain increasing, but the vibration can be suppressed more efficiently at other values.

Lu and Liu [8] investigated the primary resonance of an externally excited Duffing oscillator under feedback control with time delay. Illustrated that appropriate choice for the feedback gains and time delay can exclude the possibility of modulated motion and reduce the amplitude peak of the primary resonance. Naik and Singru [9] studied the primary, sub-harmonic and super harmonic resonances of a harmonically excited nonlinear quarter-car model with time delayed active control. Sun et al. [10] presented the effects of the time delays on chaos and bifurcation in a non-autonomous system with multiple time delays. El-Bassiouny [11–13] studied fundamental and sub-harmonic resonances of harmonic oscillation with time delay state feedback. Also, he studied vibration control of a cantilever beam with time delay state feedback. The stability and oscillation of two coupled Duffing equations with time delay state feedback are investigated.

The main aim of this paper is to introduce how to suppress the vibration in the Duffing oscillator at some values of time delay feedback. The multiple scales perturbation analysis is applied to present the analytical solution of a second-order nonlinear ordinary differential equations. Stability is studied near sub-harmonic resonance case. The numerical simulations for the system without and with time delay feedback using time history and frequency-response functions are presented. Comparison between analytical and

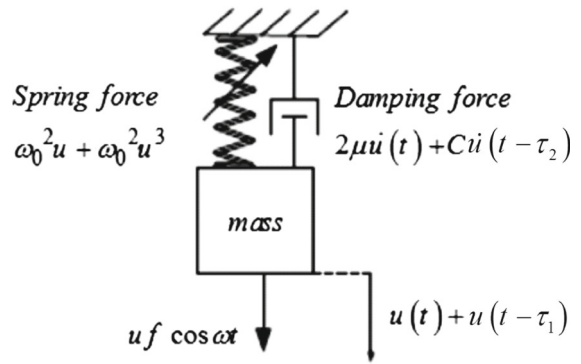


Fig. 1 Duffing system as a model of cutting [15]

numerical results is illustrated. Concluding remarks are presented.

2 Equation of the problem

The model of regenerative cutting, analyzed here, represents orthogonal cutting where the tool is model one-degree-of-freedom (1-DOF) rigid body with nonlinear, cubic stiffness characteristic. The model characterizes the process where a chip flows along the orthogonal plane and cutting edge of the tool is perpendicular to the direction of tool motion. Moreover, vibrations in u direction (perpendicular to machined surface) are the most important for the sake of finish surface quality. The presented model of orthogonal cutting can be transformed into classical Duffing oscillator with time delay feedback depicted in Fig. 1. Here, an additional parametric excitation is introduced to control vibrations generated by delayed mechanism.

The dynamics of a parametric excited Duffing oscillator under time delay control is described by the modified nonlinear differential equation given by Ref. [8] which can be simulated for the model of regenerative cutting as [15]. And the equation of the system is given by

$$\ddot{u}(t) + 2\varepsilon\mu\dot{u}(t) + \omega_0^2 u(t) + \varepsilon\omega_0^2 u^3(t) - \varepsilon u(t) + f \cos \omega t + \varepsilon B u(t - \tau_1) + \varepsilon C \dot{u}(t - \tau_2) = 0 \quad (1)$$

where $u(t)$ is generalized coordinate of the mode under consideration, the linear damping coefficient μ , ω_0 the natural frequency, ω the external excitation frequency, B and C are linear coefficients of the system, f the forcing amplitude, time delay τ and dot denotes differentiation with respect to time

3 Perturbation analysis

Applying the multiple scales method [14] we can obtain the first-order approximate solution of Eq. (1). The approximate solution will be in the form:

$$u(t, \varepsilon) = u_0(T_0, T_1) + \varepsilon u_1(T_0, T_1) + O(\varepsilon^2) \quad (2)$$

$$u(t - \tau, \varepsilon) = u_{0\tau}(T_0, T_1) + \varepsilon u_{1\tau}(T_0, T_1) + O(\varepsilon^2) \quad (3)$$

where ε is a small perturbation parameter, $T_0 = t$ and $T_1 = \varepsilon t$ are the fast and slow timescales, respectively.

The derivatives will be in the form:

$$\frac{d}{dt} = D_0 + \varepsilon D_1, \quad \frac{d^2}{dt^2} = D_0^2 + 2\varepsilon D_0 D_1 \quad (4)$$

Substitution from (2) to (4) in (1) and equating the coefficients of the same power of ε yield,

$$O(\varepsilon^0) : (D_0^2 + \omega_0^2) u_0 = 0 \quad (5)$$

$$O(\varepsilon^1) : (D_0^2 + \omega_0^2) u_1 = -2D_1 D_0 u_0 - 2\mu D_0 u_0 - \omega_0^2 u_0^3 + u_0 \frac{f}{2} \times (e^{i\omega t} + e^{-i\omega t}) - B u_{0\tau_1} - c D_0 u_{0\tau_2} \quad (6)$$

The solutions of Eq. (5) can be expressed in the form:

$$u_0 = A(T_1) e^{i\omega_0 T_0} + cc \quad (7)$$

where A is complex function in T_1 and $cc.$ is complex conjugate of the pervious term.

Expanding A_τ by Taylor series by [7] under the assumption that the product of the small parameter ε and time delay is small compared to unity, then

$$A_\tau(T_1) = A_\tau(T_1 - \varepsilon\tau) \cong A(T_1) - \varepsilon\tau A'(T_1) + \dots \quad (8)$$

where $(\cdot)' = \partial(\cdot)/\partial T_1 = \partial(\cdot)/\partial(\varepsilon t)$ because $T_n = \varepsilon^n t$

Substituting Eqs. (7) and (8) into Eq. (6), we obtain

$$\begin{aligned} &(D_0^2 + \omega_0^2) u_1 \\ &= \left[-2i D_1 A \omega_0 - 2i A \mu \omega_0 - 3\omega_0^2 A^2 \bar{A} - B A e^{-i\omega_0 T_1} - C A i \omega_0 e^{-i\omega_0 \tau_2} \right] e^{i\omega_0 T_0} \\ &\quad - \left[\omega_0^2 A^3 \right] e^{3i\omega_0 T_0} + \left[\frac{f A}{2} \right] e^{i(\omega+\omega_0)T_0} + \left[\frac{f \bar{A}}{2} \right] e^{i(\omega-\omega_0)T_0} + cc. \end{aligned} \quad (9)$$

By eliminating the secular term from Eq. (9), the first approximation solution can be written as

$$u_1 = \left[\frac{A^3}{8} \right] e^{3i\omega_0 T_0} + \left[\frac{f A}{2(\omega_0^2 - (\omega + \omega_0)^2)} \right] e^{i(\omega+\omega_0)T_0} + \left[\frac{f \bar{A}}{2(\omega_0^2 - (\omega - \omega_0)^2)} \right] e^{i(\omega-\omega_0)T_0} + cc. \quad (10)$$

Then, the reported resonance cases at this approximation order are:

- (i) Trivial resonance: $\omega = 0$
- (ii) Sub-harmonic resonance: $\omega = 2\omega_0$

4 Stability of the system

In this work, we considered the sub-harmonic resonance case $\omega = 2\omega_0$ as the worst resonance case, introducing the external detuning parameter σ as

$$\omega = 2\omega_0 + \varepsilon\sigma \quad (11)$$

Inserting Eq. (11) leads to the secular and small-divisor terms into Eq. (9) and removing these secular terms to obtain solvability for the first-order approximation

$$2i D_1 A \omega_0 = -2i A \mu \omega_0 - 3\omega_0^2 A^2 \bar{A} - B A e^{-i\omega_0 T_1} - C A i \omega_0 e^{-i\omega_0 \tau_2} + \frac{f \bar{A}}{2} e^{i\sigma T_1} \quad (12)$$

Letting $A = \frac{1}{2} a e^{i\gamma}$ in Eq. (12) and separating real and imaginary parts, we obtain the equations of the amplitude a and the phase of the motion γ

$$\begin{aligned} \dot{a} &= -\mu a + \frac{1}{2\omega_0} B a \sin \omega_0 \tau_1 \\ &\quad - \frac{1}{2} C a \cos \omega_0 \tau_2 + \frac{f}{4\omega_0} a \sin \theta \end{aligned} \quad (13)$$

$$\begin{aligned} \dot{\gamma} a &= \frac{3}{8} \omega_0 a^3 + \frac{1}{2\omega_0} B a \cos \omega_0 \tau_1 \\ &\quad + \frac{1}{2} C a \sin \omega_0 \tau_2 - \frac{f}{4\omega_0} a \cos \theta \end{aligned} \quad (14)$$

where $\theta = \sigma T_1 - 2\gamma$

For the steady-state solutions of the system we have $\dot{a} = \dot{\theta} = 0$, then we get

$$\begin{aligned} \mu a - \frac{1}{2\omega_0} B a \sin \omega_0 \tau_1 + \frac{1}{2} C a \cos \omega_0 \tau_2 \\ = \frac{f}{4\omega_0} a \sin \theta \end{aligned} \quad (15)$$

$$\begin{aligned}
 &-\frac{1}{2}a\sigma + \frac{3}{8}\omega_0 a^3 + \frac{1}{2\omega_0}Ba \cos \omega_0 \tau_1 \\
 &+ \frac{1}{2}Ca \sin \omega_0 \tau_2 \\
 &= \frac{f}{4\omega_0}a \cos \theta
 \end{aligned} \tag{16}$$

Squaring Eqs. (15) and (16) then adding the squared equations together, to obtain the frequency response equation (FRE)

$$\begin{aligned}
 &\frac{1}{4}a^2\sigma^2 + \left[-\frac{Ba^2}{2\omega_0} \cos \omega_0 \tau_1 - \frac{3}{8}\omega_0 a^4 \right. \\
 &\quad \left. - \frac{ca^2}{2} \sin \omega_0 \tau_2 \right] \sigma + \frac{1}{4\omega_0^2}B^2 a^2 + \frac{3}{8} \\
 &\quad Ba^4 \cos \omega_0 \tau_1 + \frac{9}{64}\omega_0^2 a^6 + \mu^2 a^2 - \frac{\mu Ba^2}{\omega_0} \\
 &\quad \sin \omega_0 \tau_1 + \mu Ca^2 \cos \omega_0 \tau_2 \\
 &\quad + \frac{C^2 a^2}{4} + \frac{3C\omega_0 a^4}{8} \sin \omega_0 \tau_2 - \frac{f^2}{16\omega_0^2} a^2 \\
 &\quad - \frac{1}{2\omega_0} a^2 BC \sin \omega_0 (\tau_1 - \tau_2) = 0
 \end{aligned} \tag{17}$$

To determine the stability of the steady-state solution, one lets

$$a = a_0 + a_1 \text{ and } \theta = \theta_0 + \theta_1 \tag{18}$$

where a_0 and θ_0 are the solutions of (13), (14) and a_1, θ_1 are perturbations which are assumed to be small compared to a_0 and θ_0 . Substituting (18) into (13), (14) and keeping only the linear terms in a_1 and θ_1 , we obtain

$$\begin{aligned}
 \dot{a}_1 = &\left[-\mu + \frac{1}{2\omega_0}B \sin \omega_0 \tau_1 \right. \\
 &\quad \left. - \frac{1}{2}C \cos \omega_0 \tau_2 + \frac{f}{4\omega_0} \sin \theta_0 \right] a_1 \\
 &+ \left[\frac{f}{4\omega_0} a_0 \cos \theta_0 \right] \theta_1
 \end{aligned} \tag{19}$$

$$\begin{aligned}
 \dot{\theta}_1 = &\left[\frac{\sigma}{a_0} - \frac{9}{4}\omega_0 a_0 - \frac{1}{\omega_0 a_0}B \cos \omega_0 \tau_1 \right. \\
 &\quad \left. - \frac{1}{a_0}C \sin \omega_0 \tau_2 + \frac{f}{2a_0 \omega_0} \cos \theta_0 \right] a_1 \\
 &+ \left[-\frac{f}{2\omega_0} \sin \theta_0 \right] \theta_1
 \end{aligned} \tag{20}$$

The above system can be write in the matrix

$$[\dot{a}_1 \ \dot{\theta}_1]^T = [J][a_1 \ \theta_1]^T \tag{21}$$

where $[J]$ is the Jacobian matrix of the right hand sides of (19) and (20).

The eigen values of $[J]$ are given by the following equation:

$$\lambda^2 + R_1 \lambda + R_2 = 0 \tag{22}$$

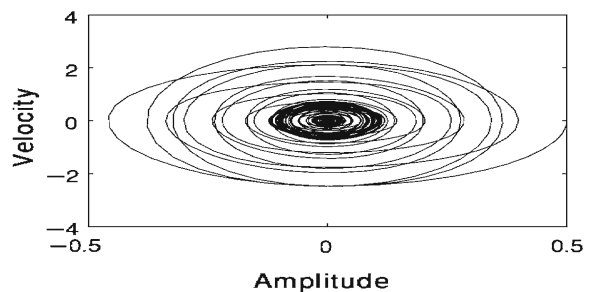
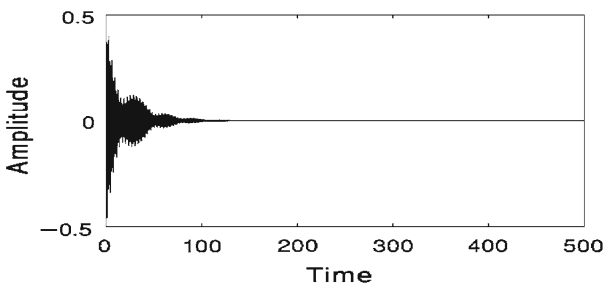


Fig. 2 Non-resonance cases for the system

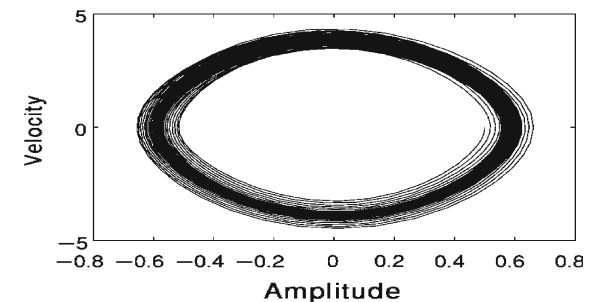
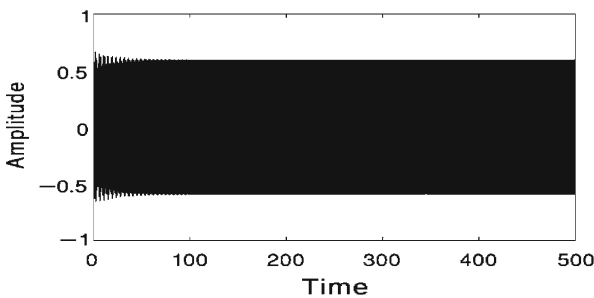


Fig. 3 Response of the system without time delay at sub-harmonic resonance case ($\omega \cong 2\omega_0$)

where R_1 and R_2 are coefficients of (23). The stability for the system is studied by examination of the eigenvalues of the Jacobian matrix of (22). The corresponding solution is stable, if the real part of each eigenvalue is negative. If the real part of any of the eigenvalues is positive, the corresponding solution is unstable.

5 Numerical simulations

The numerical solution for the differential equation (1) of the main system is obtained by applying Rung–Kutta fourth order method (RK-4) using MATLAB 7.14(R2012a) package (ode45) at sub-harmonic resonance case ($\omega = 2\omega_0$).

Figure 2 shows that the steady-state amplitude of the system and the phase-plane for the non-resonant system at selected values of the equation parameters ($\mu = 0.01$, $\omega_0 = 6$, $f = 20$, $B = 0.04$, $C = 0.06$, $\omega = 4$).

For the sub-harmonic resonance case ($\omega = 2\omega_0$) as shown in Fig. 3, the steady-state amplitude is increased to about $16.7 \times 10^6\%$ of that value shown in Fig. 2 with multi limit cycle.

5.1 Effects of time delay on system behavior

The effect of delay time on system response was studied numerically (the delay in the amplitude and the velocity of the system are equal). Figure 4a shows amplitude-delay τ_1 response curve for $\tau_2 = 0$, while Fig. 4b shows amplitude-delay τ_2 response curve for $\tau_1 = 0$. It can be observed from the above mentioned figures that, the effects of the different time delay are the same then we use $\tau_1 = \tau_2 = \tau$. It has been noticed that for $2.2 < \tau < 2.3$ the steady-state amplitude and the velocity of the system can be reduced, as shown in Fig. 4c, d. This means that the delay in this range can be used as a controller. Away from this range of time delay the steady-state amplitude and the velocity for the main system are increasing and decreasing.

5.2 Effect of various parameters for the system

The frequency response equation (FRE) given by Eq. (17) is nonlinear algebraic equations of the amplitude a against the detuning parameter σ . This equation is solved numerically as shown in figures. The curves

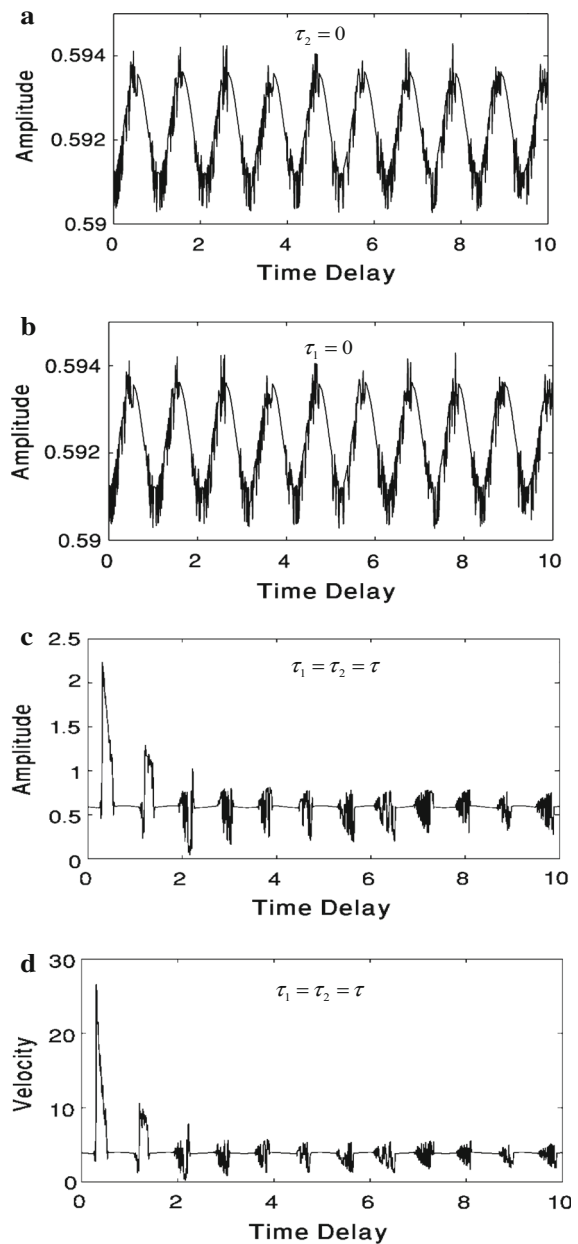
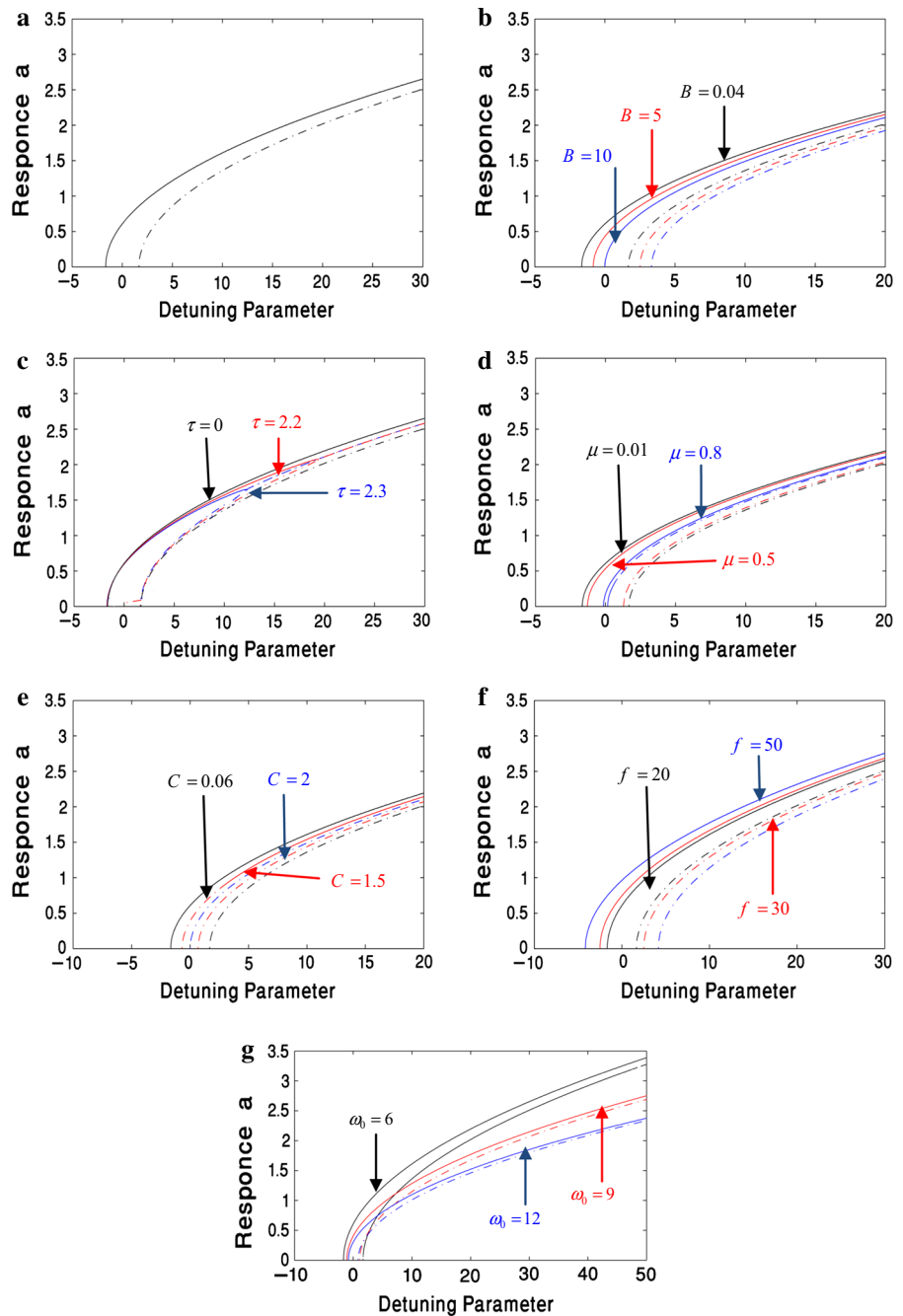


Fig. 4 Effect of delay time on system steady-state amplitude

of all these figures consist of two branches representing stable (solid line) and unstable (dashed lines) solutions. Figure 5a shows the effects of the detuning parameter σ on the steady-state amplitude of the system. Figure 5b shows that the steady-state amplitude of the system is shifted to the right for increasing value of linear parameter B . The steady-state amplitude of the system is monotonic decreasing function of the time

Fig. 5 **a** The effective of detuning parameter σ . **b** The effective of the linear coefficient B . **c** The effective of the time delay τ . **d** The effective of the damping coefficient μ . **e** The effective of linear coefficient C . **f** The effective of the forcing amplitude f . **g** The effective of natural frequency ω_0

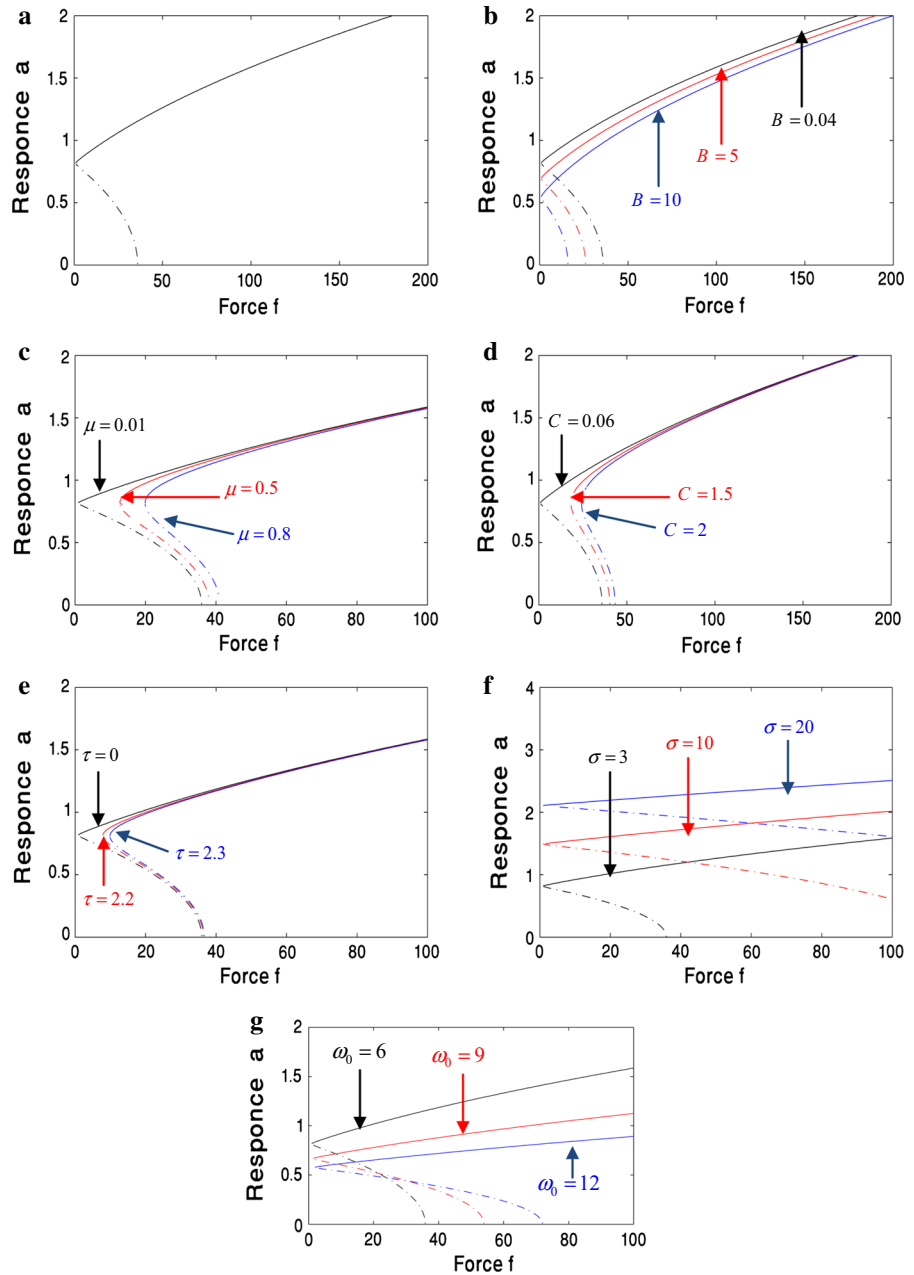


delay at the range $2.2 < \tau < 2.3$ as shown in Fig. 5c. Also, for increasing values of the damping coefficient μ and linear coefficient C the steady-state amplitude is decreased as shown in Fig. 5d, e. From Fig. 5f, the steady-state amplitude of the system is a monotonic increasing function in the parametric excitation force f . Moreover, in Fig. 5g we observed that for increas-

ing values of the natural frequency ω_0 the continuous curve is bent to right with decreasing the steady-state amplitude of the system.

Figure 6a illustrates the effects of parametric excitation f on the steady-state amplitude of the system represent stable region (solid line) and unstable region (dashed lines). From Fig. 6b, we observed

Fig. 6 **a** The effective of force without time delay. **b** The effective of linear coefficient B . **c** The effective of linear damping coefficient μ . **d** The effective of linear coefficient C . **e** The effective of the time delay τ . **f** The effective of detuning parameter σ . **g** The effective of natural frequency ω_0



that for increasing values of linear coefficient B , the continuous curve is shifted downwards with decreasing the steady-state amplitude of the system and the unstable region. Figure 6c–e shows that the steady-state amplitude is shifted to right and decreasing as the linear damping μ , nonlinear coefficient C and time delay τ are increasing. Moreover, for increas-

ing values of the detuning parameter σ , the continuous curve is shifted to right with increasing the steady-state amplitude of the system and unstable region as shown in Fig. 6f. Furthermore, Fig. 6g presented that for increase the natural frequency ω_0 is shifted downwards with decreasing the steady-state amplitude of the system.

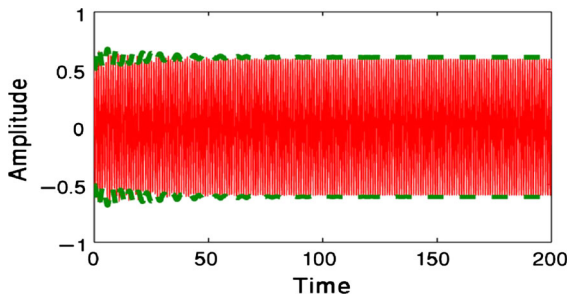


Fig. 7 Comparison between the analytical and numerical solutions of the nonlinear system *solid line* numerical solution and *dashed line* analytical solution

5.3 Comparison between analytical and numerical solution and effects of parameters

For validity, the analytical solution given by Eqs. (13), (14) is compared with the numerical solution of Eq. (1) for nonlinear dynamical system as shown in Fig. 7 by using the chosen values of the system parameters which presented graphically in Fig. 4.

From Fig. 8a, b, it can be seen that the amplitude is monotonic decreasing function on the coefficients B and C, which is a good agreement with Figs. 5b, e and 6b, d. Also from Fig. 8c we find that the steady-state amplitude has peak and then increase at resonance case at subharmonic resonance case, which is studied in the frequency response equations.

Fig. 8 **a** The effective of the linear parameter B. **b** The effective of the linear parameter C. **c** Response of the natural and excitation frequencies

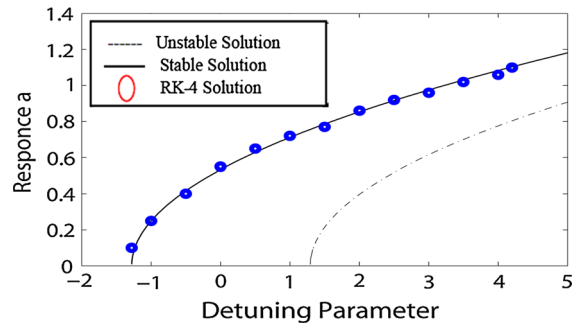
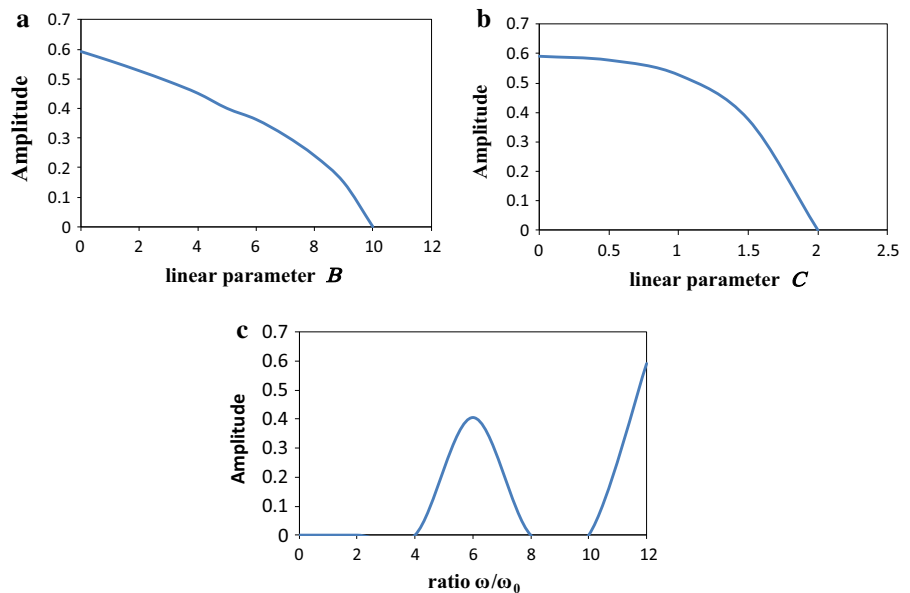


Fig. 9 Validated between RK-4 and FRC

5.4 Validated between RK-4 and FRC

Figure 9 clarifies that the validation between the steady-state amplitude (u) using the numerical solution (RK-4) of Duffing Oscillator Eq. (1) (marked as small circles) and the steady-state amplitude (a) using the frequency response equation (FRC) given by Eq. (17). Figure 9 presents a good agreement with the amplitude using RK-4 at the same value for the detuning parameter σ .

5.5 Comparison with published work

1. Reference [8] studied Duffing oscillator under feedback control with time delay subjected to external force at primary internal resonance case ($\omega \approx \omega_0$).

2. This paper illustrates Duffing oscillator system with time delay feedback control under parametric excitation force at sub-harmonic resonance case ($\omega \cong 2\omega_0$). We succeeded to reduce the steady-state amplitude of the system using time delay control in the range $2.2 < \tau < 2.3$. Moreover, numerically the stable and unstable regions are defined when studying the effects of the selected parameters.

6 Conclusions

Duffing oscillator system with time delay feedback has been considered and solved under parametric excitation force. The time delay can be used as a controller for reduction of the amplitude of the nonlinear system. The MSPT method has been applied to determine the frequency response equations. Then, it is observed from the numerical study of the stability.

- 1) The worst behavior of the main system occurs at sub-harmonic resonance case $\omega \cong 2\omega_0$.
- 2) Time delay can be used as a control parameter for suppressing the vibration of the dynamical system in the ranges is $2.2 < \tau < 2.3$ as show in Fig. 4.
- 3) The steady-state amplitude of the main system is monotonic increasing function of the excitation force f .
- 4) The steady-state amplitude of the main system is monotonic decreasing functions of the coefficient C , natural frequency ω_0 and damping coefficient μ .

References

1. El-Bassiouny, A.F., El-kholy, S.: Resonances of a nonlinear SDOF system with time-delay in linear feedback control. *Phys. Scr.* **81**, 015007 (12pp) (2010)
2. El-Ganaini, W.A.A., Elgohary, H.A.: Vibration suppression via time-delay absorber described by non-linear differential equations. *Adv. Theor. Appl. Mech.* **4**(2), 49–67 (2011)
3. El-Gohary, H.A., El-Ganaini, W.A.A.: Vibration suppression of a dynamical system to multi-parametric excitations via time-delay absorber. *Appl. Math. Model.* **36**, 35–45 (2012)
4. Saeed, N.A., El-Ganaini, W.A., Eissa, M.: Nonlinear time delay saturation-based controller for suppression of nonlinear beam vibrations. *Appl. Math. Model.* **37**, 8846–8864 (2013)
5. El-Sayed, A.T., Bauomy, H.S.: Vibration control of helicopter blade flapping via time-delay absorber. *Meccanica* **49**, 587–600 (2014)
6. Nbandjo, B.R.N., Tchoukuegno, R., Wofo, P.: Active control with delay of vibration and chaos in a double-well Duffing oscillator. *Chaos Solitons Fractals* **18**, 345–353 (2003)
7. Zhao, Y.Y., Xu, J.: Effects of delayed feedback control on nonlinear vibration absorber system. *J Sound Vib.* **308**, 212–230 (2007)
8. Lu, W., Liu, Y.: Vibration control for the primary resonance of the Duffing oscillator by a time delay state feedback. *Int. J. Nonlinear Sci.* **8**(3), 324–328 (2009)
9. Naik, R.D., Singru, P.M.: Resonance stability and chaotic vibration of a quarter-car vehicle model with time-delay feedback. *Commun. Nonlinear Sci. Numer. Simul.* **16**, 3397–3410 (2011)
10. Sun, Z., Xu, W., Yang, X., Fang, T.: Effects of time delays on bifurcation and chaos in anon-autonomous system with multiple time delays. *Chaos Solitons Fractals* **31**, 39–53 (2007)
11. El-Bassiouny, A.F.: Fundamental and subharmonic resonances of harmonically oscillation with time delay state feedback. *Shock Vib.* **13**, 65–83 (2006)
12. El-Bassiouny, A.F.: Vibration control of a cantilever beam with time delay statefeedback. *Verlag der Zeitschriftfür-Naturforschung61a*, 1–1220 (2006)
13. El-Bassiouny, A.F.: Stability and oscillation of two coupled Duffing equations with time delay state feedback. *Phys. Scr.* **75**, 726–735 (2006)
14. Nayfeh, A.: *Perturbation Methods*. Wiley, New York (1973)
15. Rusinek, R., Weremczuk, A., Kecik, K., Warminski, J.: Dynamics of a time delayed Duffing oscillator. *Int. J. Non-Linear Mech.* **65**, 98–106 (2014)